AN ABSTRACT OF THE THESIS OF

Matthew L. Chin for the degree of Honors Baccalaureate of Science in Electrical Engineering presented on June 5th, 2006. Title: A Fabrication Study of Surface Acoustic Wave Devices for Magnetic Field Detection

Abstract Approved:

_____

Pallavi Dhagat

Surface acoustic wave (SAW) sensors are versatile devices that can be configured to sense a variety of measurands such as temperature and pressure. The potential use of surface acoustic wave devices for magnetic field detection is explored in this study. Compared to current magnetic field sensors, a sensor based on a SAW delay-line could theoretically achieve a substantially higher sensitivity. In addition to this, such a device could potentially be interrogated wirelessly and act passively consuming no power, opening the doors for numerous application possibilities.

A proposed basic design for a SAW magnetic wave sensor is presented along with a fabrication process to manufacture such a device. Using a common SAW delay-line as the basis of the design, material and component selection is justified. A lithium niobate piezoelectric substrate is used as the foundation of the device, with the interdigital transducers fabricated with aluminum. The stimulus-detecting component of the device is a magnetostrictive nickel thin film. A standard microelectronic fabrication process flow was designed and implemented in creating prototype devices using the materials and components described. The fabricated devices are described and issues arising from fabrications are also discussed.

Key Words: Surface Acoustic Wave, SAW, magnetic sensors, magnetic fields, delay line

Corresponding E-mail Address: chinm@engr.oregonstate.edu

A Fabrication Study of a Surface Acoustic Wave Device for Magnetic Field Detection

by

Matthew L. Chin

A PROJECT

Submitted to

Oregon State University

University Honors College

In partial fulfillment of

the requirements for the

Degree of

Honors Baccalaureate of Science in Electrical Engineering (Honors Scholar)

Presented June 5th, 2006

Commencement June 2006

Honors Baccalaureate of Science in Electrical Engineering project of Matthew L. Chin
presented on June 5th, 2006

APPROVED:

_____
Mentor, representing Electrical Engineering – Materials and Devices

_____
Committee Member, representing Electrical Engineering – Materials and Devices

_____
Committee Member, representing Electrical Engineering – Materials and Devices

_____
Committee Member, representing Electrical Engineering – Mixed Signal Integration

_____
Dean, University Honors College

I understand that my project will become part of the permanent collection of Oregon State University, University Honors College. My signature below authorizes release of my project to any reader upon request.

_____
Matthew L. Chin, author

ACKNOWLEDGEMENTS

I would like to acknowledge the invaluable contributions and guidance of Professor Pallavi Dhagat, who gave me the technical background and the encouragement needed to complete this project. I would like to also acknowledge the help of Professor Albrecht Jander, Professor Tom Plant, and Chris Tasker for their advice and guidance. Without the guidance and advice they provided, this project would have been far less successful, with many more challenges to overcome. I cannot thank Rick Presley, Hai Chiang and Manfred Dittrich enough for their constant effort and assistance, spending many days and sometimes late nights with me to get those devices fabricated. Finally, I would like to thank the staff of the Oregon State University Honors College and its Dean for the constant encouragement. Without that, I would not have mentally made it through. Thank you.

Table of Contents

List of Figures

List of Tables

A Fabrication Study of a Surface Acoustic Wave Device for Magnetic Field Detection

1. Introduction

Acoustic wave devices and in particular, surface acoustic wave devices, have been used in commercial applications since the 1970's [1]. The purpose of this paper is to investigate the potential and feasibility of using a surface acoustic wave delay-line with a nickel magnetostrictive thin film layer for detecting magnetic fields. In recent years, there has been an explosive growth in research in surface acoustic wave (SAW) devices for sensor uses. The research has demonstrated the versatility and the vast capabilities of this particular technology. Inherently, SAW devices are capable of detecting changes in temperature, pressure, strain, torque, and mass loading [2, 3]. Through the use of a thin film located in between the interdigital transducers of a SAW delay line, it is possible to detect the presence of a variety of chemical vapors, biological matter, electric fields and potentially, magnetic fields [2, 3]. The primary focus of this paper will involve justifying the ability of a SAW device to detect magnetic fields and describe a method for fabricating a SAW magnetic field sensor.

Following the introduction in Chapter 1, the paper is structured as follows: Chapter 2 presents a brief history of surface acoustic wave devices. Chapter 3 describes the proposed configuration of the SAW device and the physics of how the device works. Chapter 4 discusses the material science involved with the fabrication of the proposed SAW sensor and justifies the choices made for material selections. Chapter 5 details the microelectronic fabrication steps used to develop the proposed SAW device. Chapter 6

discusses the potential applications and advantages for the SAW magnetic field sensor. A brief comparison between the SAW magnetic field sensor and current sensors on the market is also provided in this chapter. Chapter 7 provides the fabrication results along with conclusions and potential future research stemming from this fabrication study.

2. History

The concept of surface acoustic waves, also known as Rayleigh waves, can be traced back to Lord Rayleigh in 1885 as he analyzed surface waves in solids. He applied the results of his studies to the earth's seismic activity [1, 3]. Less than eight decades later, in 1963, two scientists independently published the first papers on planar SAW transducers. J. H. Rowen and S. K. Settig patented the precursor to what is now the predominant SAW device design, the planar SAW pulse compressor [1, 4]. Concurrently, W.S. Mortley created and demonstrated the first transducers that made use of interdigital electrodes [3]. The first experimental results were collected and published, from what could be considered the first modern SAW device in 1965. These experiments were performed on SAW devices created by R. M. White and F. W. Voltmer [1, 3, 5]. Their experiment involved generating and receiving surface waves on a quartz piezoelectric substrate using interdigital transducers.

Since then, SAW devices have found commercial applications in a variety of areas. In the 1970's, the SAW devices were primarily used for pulse compression filters in radar systems funded by the United States military [1]. SAW devices were found to be useful as band pass filters as well. In the 1980's and 1990's, SAW devices found a niche as oscillators, low pass filters, band pass filters, convolvers, and resonators in the new microelectronics field [1, 5]. Cell phones, video recorders, computers and televisions are some of the more prominent consumer electronics to have SAW filters and oscillators incorporated into them [1, 6]. By the mid 1990's and 2000's, a renewed focus on SAW research brought light back on this technology in the field of sensors. Scientists are

finding ways to exploit the properties of SAW devices to be used as sensors in a variety of applications for eventual commercial release. Recently, some of these sensor technologies have made their debut as fleshed-out products. Magnetic field detection is one of the many potential SAW device applications that are currently being researched.

3. SAW Magnetic Field Sensor Description

The proposed surface acoustic wave (SAW) device for detecting magnetic fields is a SAW sensor based on the delay-line configuration. SAW sensors are a class of sensors which make use of transducers that convert electrical signals into acoustic waves and vice versa. In the case of a SAW magnetic field sensor, the measurand is magnetic field, which produces a stress on a magnetostrictive thin film on the SAW substrate. As a magnetostrictive material, nickel transduces or converts magnetic energy into mechanical energy. An electrical signal is inputted on one side of the sensor, which is then converted into a surface acoustic wave (also called a Rayleigh Wave). Rayleigh waves generated on the surface of a solid are similar to ripples on the surface of water. When the acoustic wave reaches the other side of the device, it is converted back into an electrical signal to be detected by analysis tools and circuitry. Depending on the externally applied magnetic field, the subsequent stress on the nickel film changes the velocity or time delay of the propagating SAW. This is caused by the strain change in length per unit length on the nickel thin film, which changes the piezoelectric substrate strain in between the input and output interdigital transducers. This in turn changes the electrical signal (the voltage amplitude, the voltage phase, or both) that is detected on the other side of the sensor.

3.1 SAW Delay-Line Devices

The two-port SAW delay-line configuration consists of a rectangular piezoelectric substrate area with two interdigital transducers (IDTs) placed on top of the substrate, located on either ends of rectangular area. One of the interdigital transducers is

connected to an alternating or oscillating voltage source (the input interdigital transducer). The other transducer is connected to signal conditioning circuitry and signal detection circuitry (the output interdigital transducer). Figure 1 details a general SAW delay-line device. When an oscillating voltage is applied between alternately connected (interleaved) electrodes, a periodic electric field is imposed on the piezoelectric substrate crystal structure. A physical, periodic strain field is created due to this applied voltage. This strain field in turn, generates a surface acoustic wave across the surface of the piezoelectric substrate. The surface waves propagate in the substrate and are subsequently launched in both directions from the generating interdigital transducer perpendicular to the interdigital transducer fingers (as shown in Figure 1).

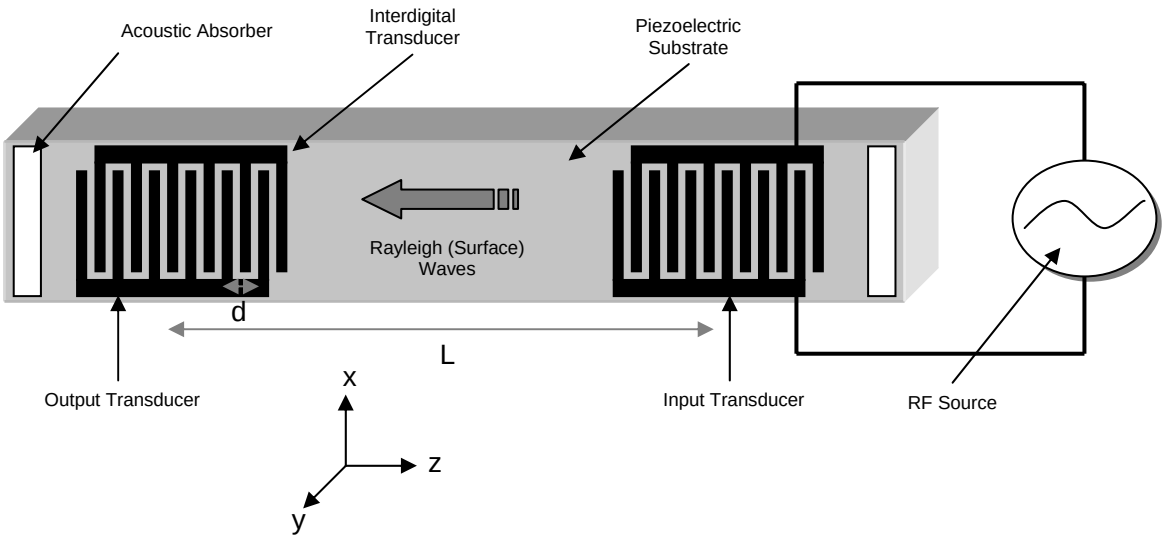

Figure 1 - Diagram of a two-port SAW delay-line device

The transducers are most efficient in converting electrical signals into mechanical surface acoustic waves when the SAW wavelength (λ) matches the periodicity of the interdigital transducer fingers [3, 4, 5, 7], which is defined as the distance between a pair of alternating electrodes and their associated gaps. This is shown in Figure 2. If the

wavelength of the surface acoustic waves and the periodicity of the transducer fingers match, then the SAW delay-line are at the synchronous frequency, defined as the frequency at which the applied voltage most efficiently produces mechanical surface acoustic waves. The equation for determining the optimal voltage frequency to apply between the electrodes is given by Equation 1 below.

$$f_0 = \frac{v_0}{d} \qquad \text{(Equation 1)}$$

In Equation 1, 'f_0' is the synchronous frequency, 'v_0' is the SAW propagation velocity, and 'd' is the periodicity of the transducer fingers [3, 4, 5, 7].

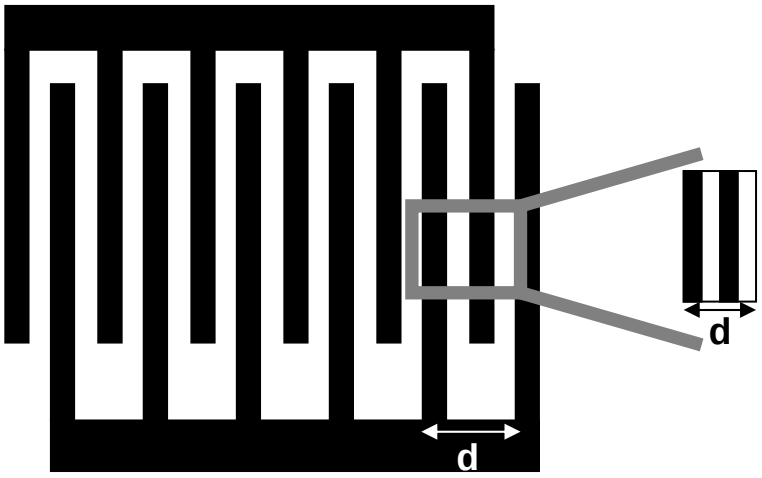

Figure 2 – Interdigital transducer (IDT) spacing definition

At the receiving interdigital transducer, the opposite occurs. The mechanical surface acoustic waves in piezoelectric substrate have an associated wave potential (Φ) [3, 5]. When the mechanical SAWs encounter a receiving interdigital transducer, the strain field and the associated wave potential of the wave induces a current flow between the two alternating electrodes that make up the transducer. This current flow can then be picked up by the external detection circuit.

When a SAW propagates at the input transducer and then travels to the output transducer at a velocity characteristic of the piezoelectric substrate, there will be a time delay between the generation of the surface wave at the input transducer and its reception at the output transducer. This time delay can be determined from Equation 2.

$$t_d = \frac{l}{v_0} \qquad \text{(Equation 2)}$$

Equation 2 variables are defined as follows: 't_d' is the time delay, 'l' is the distance between the center points of the input transducer and the output transducer, and 'v_0' is the SAW propagation velocity characteristic of the piezoelectric substrate [6, 7]. This time delay can be potentially measured to detect change in relation to a measurand. A measurand that induces a strain in the piezoelectric substrate will consequently influence the surface wave, changing its velocity and inversely changing the time delay [3, 5, 6].

What differentiates SAW sensors and devices from other acoustic wave devices is the fact that they make use of strictly surface waves in solids. The energy associated with Rayleigh (or surface) waves are confined to the surface. The wave displacement profile is dependent on the depth into the crystal. Surface waves that are deeper within the crystal possess substantially less energy than those at the surface, varying by approximately $e^{-2\pi y/\lambda}$ where 'y' is the depth of the surface wave, and 'λ' is the wavelength of the SAW [5]. The majority of the wave energy is contained well within one SAW wavelength from the surface of the substrate, effectively acting like a waveguide. It should be noted that the sensitivity to surface perturbation is substantially increased in SAW devices because of this surface confinement of the waves.

All SAW sensors make use of the electrical-mechanical wave coupling of piezoelectric materials, generating surface acoustic waves using interdigital transducers. However, there is an inherent issue with this arrangement. Due to the bidirectional nature of propagating surface waves launched from the generating or input IDT, half of the energy coupled is launched in the wrong direction, opposite of where the receiving or output IDT is located. When the wave reaches the edge of the delay-line device, reflections occur, which in turn distort the frequency response at the output transducer [3, 8]. To address this source of interference, acoustic absorbers are used. Acoustic absorbers absorb the surface waves launched by the signal generating transducer that are going in the opposite direction of the output transducer. Usually the ends of a SAW sensor are coated with acoustic absorbers to reduce interference caused by reflecting waves. Various types of acoustic absorbers have been developed. The most common types are usually applied manually. Waxes and epoxies are common types of acoustic absorbers for higher frequencies. Silicon and polyimide are other acoustic absorbers being researched [8]. The ability to pattern them during the fabrication of the SAW device using standard microelectronic fabrication processes gives advantage to the latter two types of acoustic absorbers.

3.2 Magnetic Field Detection with a SAW Delay-Line Device

To detect an applied external magnetic field, the proposed SAW magnetic field sensor makes use of a magnetic thin film placed in between the input transducer and the output transducer of the SAW delay-line. Ferromagnetic materials such as nickel, cobalt and iron, possess a magnetic field-dependent elastic constant. This elastic constant

describes the elasticity or stiffness of a material, and is usually synonymous with Young's modulus (usually given the symbol 'E' and units of Pa). A high Young's modulus usually means that the there is a relatively high length change when tension is applied to the magnetic thin film [9]. Strain and subsequently, small length changes in a non-magnetized (soft magnetic material) ferromagnetic thin film, are caused by either a strictly mechanical elastic expansion that occurs in most solids or an expansion resulting from an external magnetic field stressing the orientation of magnetic domains, known as magnetostriction. It is the second cause of thin film strain and length change that is pertinent to detecting magnetic fields. Magnetostriction is responsible for the fact that in ferromagnetic materials, Young's modulus depends on the amplitude of strain and on the intensity of magnetization.

The tension on any thin film, magnetic or non-magnetic, will put a strain on the material, but for magnetic thin films, the strain on the thin film can be increased due to an externally applied magnetic field. The external magnetic field affects the elasticity of the magnetostrictive thin film, changing the length of the material. Since the magnetostrictive thin film is directly adhered to the piezoelectric substrate, a strain develops between the two materials. When a SAW propagates through the magnetic thin film, the magnetoelastic coupling between the magnetic film and the SAW changes the velocity of the SAW. The change of SAW velocity is caused by the change in the magnetostrictive thin film strain on the piezoelectric substrate. This effect is called the ΔE effect [10, 11]. This change can be detected through the use of a network analyzer, detecting the change in velocity, a change in time delay, or the phase change of the SAW. Figure 2 displays the proposed SAW magnetic field sensor.

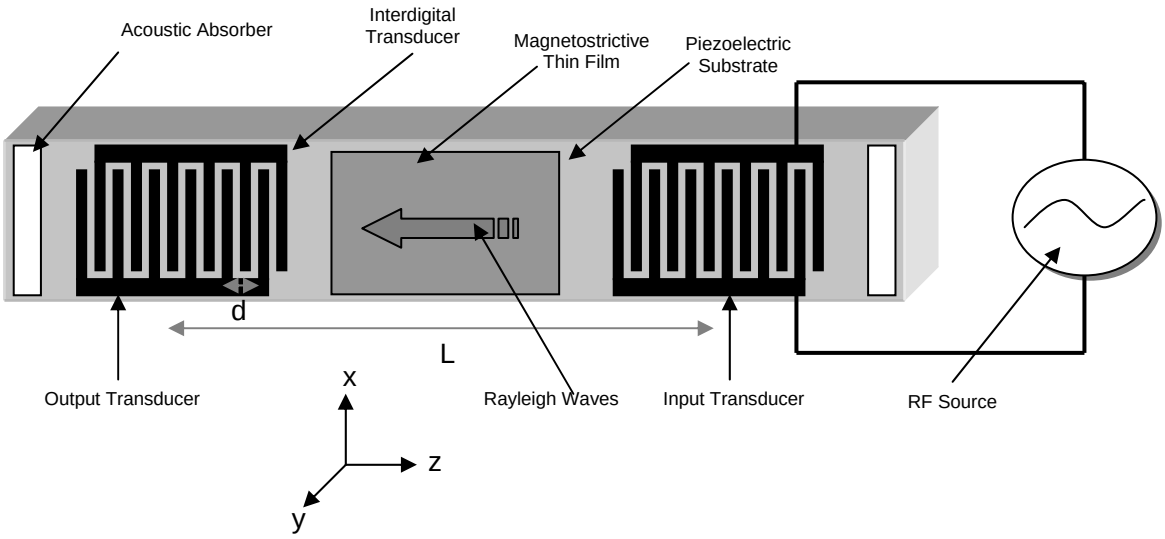

Figure 3 - Diagram of proposed SAW Magnetic Field Sensor design

There are limits to the ΔE effect, as the strain caused by an external magnetic field will reach a saturation point. This point is reached when the strain difference between the magnetostrictive thin film with no external field applied to it and the magnetostrictive thin film with an extremely large external field applied to it is equal to λ_s [9]. λ_s is a constant dependent on the magnetostriction properties of the ferromagnetic material. In general, the ΔE effect is largest for materials with large magnetostriction and small internal strain such as annealed nickel.

It should also be noted that the change in Young's modulus (ΔE effect) is not only dependent on the mechanically applied tension and the external magnetic field for magnetostrictive thin films. Temperature also has affects the elasticity of the thin film, adding another layer of complexity [9].

4. Material Selection and Properties

Surface acoustic wave delay-lines are composed of two primary components. The piezoelectric substrate and the interdigital transducers in combination, form the core of all modern SAW devices. The selections of materials that make up these two components are critical to the application and performance of a particular SAW device. For the SAW magnetic sensor, an additional component must be considered as well. The magnetic film material must also be carefully selected for its properties, corresponding to the requirements of the device.

4.1 Piezoelectric Substrate

Important material properties that must be considered in selecting a piezoelectric substrate include the electro-mechanical coupling coefficient, the temperature coefficient, the inherent wave propagation through the material, the functional frequency range, and maximum temperature tolerance. These properties are all based upon the piezoelectric material substrate and how the substrate is cut and subsequently, how the lattice structure is arranged. Table 2 provides a list of some common piezoelectric materials that could be used in SAW devices, and in particular, SAW delay line devices.

Material	***Orientation***	***Velocity***	***Temperature Coefficient***	***Coupling Coefficient***	***Cost***
(Name)	(Axis)	(m/s)	(ppm/°C)	(%)	(Qualitative)
Quartz	Y, X	3159	-24	0	Low
Quartz	Y ST, X	3159	0	0.16	Low
Lithium Tantalate	Y, Z	3230	35	0.74	Medium
Lithium Tantalate	167° Y, X	3394	64	N/A	Medium
Lithium Niobate	Y, Z	3488	94	4.6	High
Lithium Niobate	128° Y, X	3992	75	5.6	High
Langasite	Y, X	2330	38	0.37	High

Table 1 - Common Piezoelectric Substrate Properties from University of Central Florida

The wave velocity (also called the propagation velocity) is the speed (m/s) of the surface wave through the solid medium. This is directly associated with the piezoelectric substrate material and its orientation. The orientation is given by the axis in the direction in which the substrate was cut, followed by the axis of wave propagation. Both of the axes are given with respect to the crystal lattice structure and the faces of the crystal. This property plays a crucial role, as it is one of properties that dictate the synchronous frequency of a SAW sensor, which is the frequency for which the piezoelectric substrate achieves the maximum efficiency in converting the electrical signals into mechanical surface waves and vice-versa.

The electro-mechanical coupling coefficient corresponds to a material's ability to convert electrical or radio frequency signals into a mechanical surface acoustic wave when facilitated by the appropriate transducer. Substrate materials with a higher coupling coefficient make better sensors since the output signal amplitude will be more representative of the input signal amplitude (reduced signal loss and distortion). The coupling coefficient is usually given in terms of percentage [3, 7].

The temperature coefficient associated with a material presents a unique issue for selecting an appropriate substrate and possesses units of [ppm/K] or [ppm/°C]. Materials

with a small or zero temperature coefficient are not affected by temperature change, or are affected very little (i.e. the substrate does not react or strain). Materials with a large temperature coefficient are very much affected by shifts in temperature and the results are inherently incorporated in the output signal of a SAW sensor [3, 7]. A large temperature coefficient is seen as a benefit when temperature is the factor or measurand being sensed, but if a SAW sensor is made to detect a measurand other than temperature, having a temperature coefficient of any size introduces error into the measurement as it will affect the substrate strain, and thus affect the surface wave propagation. The operating frequency range that one can make use of on a particular SAW sensor is also dependent directly upon the substrate material chosen [2, 3, 6, 7].

These properties vary not only from a difference in piezoelectric substrate material, but also from the angular cut of the piezoelectric substrate material. Since piezoelectric substrates possess a crystalline structure, the angle and axis of propagation really matters, affecting both the wave propagation velocity and all of the other key properties described. The crystalline structure affects how the substrate compresses and strains, thus affecting the wave propagation [3]. This is described as the orientation in Table 1.

Choosing an appropriate substrate with the appropriate angular cut is a critical step in the design of a SAW-based sensor. For the SAW magnetic field sensor, a lithium niobate piezoelectric substrate with a Y, Z orientation was chosen. Lithium niobate possesses a higher coupling coefficient compared to quartz, lithium tantalate, and langasite, which is desired for creating surface waves with IDTs (as displayed in Table 2). Lithium niobate and quartz are well-known and common substrates used, whereas

langasite and lithium tantalate are relatively new materials with little characterization data collected on them at the time of this study. The Y-Z orientation of lithium niobate was selected over the Y-Z 128º oriented lithium niobate because of availability. Fewer vendors carried the Y-Z 128 º oriented version of lithium niobate wafers, whereas the Y-Z oriented wafers were more numerous and in vendor inventories.

The ability to fabricate devices on the substrate using standard microelectronic fabrication techniques, a high coupling coefficient, and high availability from vendors were the primary factors used to determine the optimal substrate to select for the foundation of the SAW magnetic field sensor. Lithium niobate tends to meet these three requirements well. There is a downside to lithium niobate. The substrate tends to be brittle and susceptible to thermal shock [12] and it possesses a high temperature coefficient, but even so, the advantages of the material outweigh its shortcomings, which can be worked around through proper processing.

4.2 Interdigital Transducers

The interdigital transducers (IDTs) consist of comb-shaped electrodes used in tandem. The comb-shaped electrodes are meshed together through their long, alternating fingers as shown in Figure 2 in Section 2. These alternating fingers of the comb-shaped electrodes cause strain or compression on the surface of the piezoelectric substrate when a voltage differential is applied between them. A highly conductive, low cost material that adheres well to the substrate and is relatively easy to deposit during device fabrication is a requisite for the construction of the IDTs for SAW devices.

Common metals used in modern microelectronic fabrication include copper (Cu), aluminum (Al), gold (Au), tungsten (W), and titanium (Ti). All of the metals listed above possess decent conductivity properties necessary for accommodating the input electrical signals. Aluminum, titanium and copper adhere well to most substrates [13], making good electro-mechanical coupling in most cases as well. Gold and tungsten on the other hand, possesses poor substrate adhesion [13] and requires another metal layer such as titanium or chromium to attach to the substrate. Deposition techniques that can be used also differ between materials. Copper, aluminum, gold, and titanium can be deposited onto the substrate using evaporation, sputtering or chemical vapor deposition (CVD) techniques [14]. Tungsten can only be deposited using either sputtering or chemical vapor deposition techniques, since the boiling point of tungsten is too high for the use of evaporation techniques [15]. The metal deposition method used for processing the SAW magnetic field sensor is described in Chapter 5, which discusses device fabrication techniques. Some of the pertinent properties of these three materials are given in Table 3 below. The material cost differs between the metals as well, with aluminum and copper costing substantially less than gold. Titanium and tungsten have a price that is in between the other metals.

Metal	***Substrate Adherence***	***Electrical Resistivity***	***Boiling Point***	***Cost***
(Name)	(Qualitative)	(μΩ-cm)	(K)	(Qualitative)
Copper	Good	1.7	3200	Low
Aluminum	Good	2.65	2792	Low
Gold	Poor	2.2	3129	High
Tungsten	Average	5.0	5828	Mid
Titanium	Good	50	3560	Mid

Table 2 - Table of pertinent metal properties from webelements.com and from sources [12] and [14]

The interdigital transducers for the SAW magnetic field sensor were fabricated out of aluminum. Aluminum possesses the requisite low resistivity along with good adherence properties facilitating good electro-mechanical coupling. Although copper possesses good adherence to substrates in general, copper has the tendency to diffuse into substrate materials, contaminating them and changing their inherent properties. Aluminum also has a low melting temperature meaning that faster and simpler metal deposition techniques such as thermal evaporation can be used in the fabrication process. Tungsten was eliminated from the selection process due to its extremely high melting point, meaning that only special CVD deposition techniques could be used to deposit tungsten, making it undesirable. The low price of aluminum and its common standard status in university fabrication facilities across the country makes the material easy to find with low lead times.

4.3 Magnetic Thin Film

The magnetic thin film located in between the IDTs of the SAW delay-line device is the final critical component necessary for creating a SAW-based magnetic field sensor. As discussed in Section 3.2, the magnetic thin film is the component of the SAW magnetic sensor that does the actual detecting of the measurand, which in this case is magnetic field. The elastic properties of the ferromagnetic material affect the velocity of the SAW traversing between the two IDTs. This change in velocity can be detected with a network analyzer used as the signal conditioning and detection circuitry.

The most common ferromagnetic materials include iron, nickel, and cobalt. For the fabrication of a SAW magnetic field sensor, the desired properties include the following: The material must have a relatively high value for Young's modulus (high longitudinal strain) and a low boiling point. It must be useable in microelectronic fabrication processes; it must have a high permeability; and it must be very magnetostrictive. A high Young's modulus value means the material can be longitudinally strained more. High magnetic permeability allows for higher magnetizations that respond linearly to applied magnetic fields. Good magnetostrictive properties allude to high dimensional changes as an external magnetic field is applied, increasing the $\Delta E/E$ ratio. Table 3 compares these various properties for the three common ferromagnetic metals [11]. Ferromagnetic metals with lower boiling points make the one of the easiest metal deposition process, thermal evaporation, possible.

Metal	***Young's Modulus***	***Boiling Point***	***Max Magnetic Permeability***	***Magnetostrictive Properties***
(Name)	(GPa)	(K)	(No units)	(Qualitative)
Iron	211	3134	5000	Low
Nickel	200	3186	600	High
Cobalt	209	3200	250	Very High

Table 3 - Table of properties for common ferromagnetic materials

For the SAW magnetic field sensor design, nickel was selected for the magnetic thin film due to its high magnetostrictive properties and decent maximum permeability. All of the common ferromagnetic metals possessed similar Young's modulus values and similar boiling points. All three metals can be used in standard microelectronic fabrication. Iron possesses a very high magnetic permeability, but since the film will be

exposed to standard atmospheric conditions, a high possibility of rusting restricts its usefulness. Cobalt was not chosen due to its low magnetic permeability in comparison to nickel. Nickel seems to be the optimal material candidate among the common ferromagnetic metals.

5. Device Fabrication

The SAW magnetic field sensor designed for this experiment was developed using industry standard microelectronic fabrication techniques including standard photolithography, wet etch, and thermal evaporation. This chapter describes the processes and the manufacturing parameters used to create the SAW magnetic field sensor prototype.

5.1 Process Flow Overview

As described in previous chapters, the SAW magnetic field sensor is based off of a SAW delay-line device with a magnetostrictive nickel film deposited in between the input transducer and the output transducer. To create the SAW device, a piezoelectric substrate wafer is used as the starting point. In the case of this device design, lithium niobate was the chosen substrate for reasons described in Section 4.1.

The wafer is first cleaned using the Acetone-Methanol-Deionized Water (AMD) or Acetone-Isopropyl Alcohol-Deionized Water (AID) cleaning procedure as described in the next section. Following the clean, aluminum is uniformly deposited on one entire face of the wafer for the creation of the interdigital transducers. Photoresist is then spun on top of the aluminum deposit in preparation for the photolithography process. A photo-mask is used to place down the interdigital transducer pattern onto the aluminum-deposited piezoelectric substrate. Through the use of an aligner, the photoresist layer on the wafer is exposed to UV light. All portions of the photoresist on the wafer not

protected by the mask are then washed away with the use of a developer solution, exposing the aluminum metal layer underneath. The exposed aluminum is etched away through the use of an acid bath, leaving aluminum metal only where the photoresist remained. Once the etching process is complete, the protective layer of photoresist is removed with acetone.

The piezoelectric wafer now has etch-patterned interdigital transducers made out of aluminum metal. The photo-masks used for this experimental procedure contained between two (2) and three (3) different IDT spacings and designs within a square-inch area. At this point, the device possesses the full functionality of a two-port surface acoustic wave delay-line. To add the magnetic field detection abilities to this sensor device, a thin film of magnetostrictive nickel has to be added between the two interdigital transducers.

The AMD/AID cleaning procedure is repeated in preparation for another metal deposition. The wafer with the SAW delay-line structures is brought back for another thermal evaporation. This time, a shadow mask is used to protect all portions of the wafer where the nickel thin film is not to be placed, and to ensure that the nickel film is placed only in the regions in between the IDTs. Nickel is deposited in between the IDT, completing the fabrication process after another AMD/AID cleaning procedure is performed. Figure 3 provides diagrams the process flow in wafer cross sections.

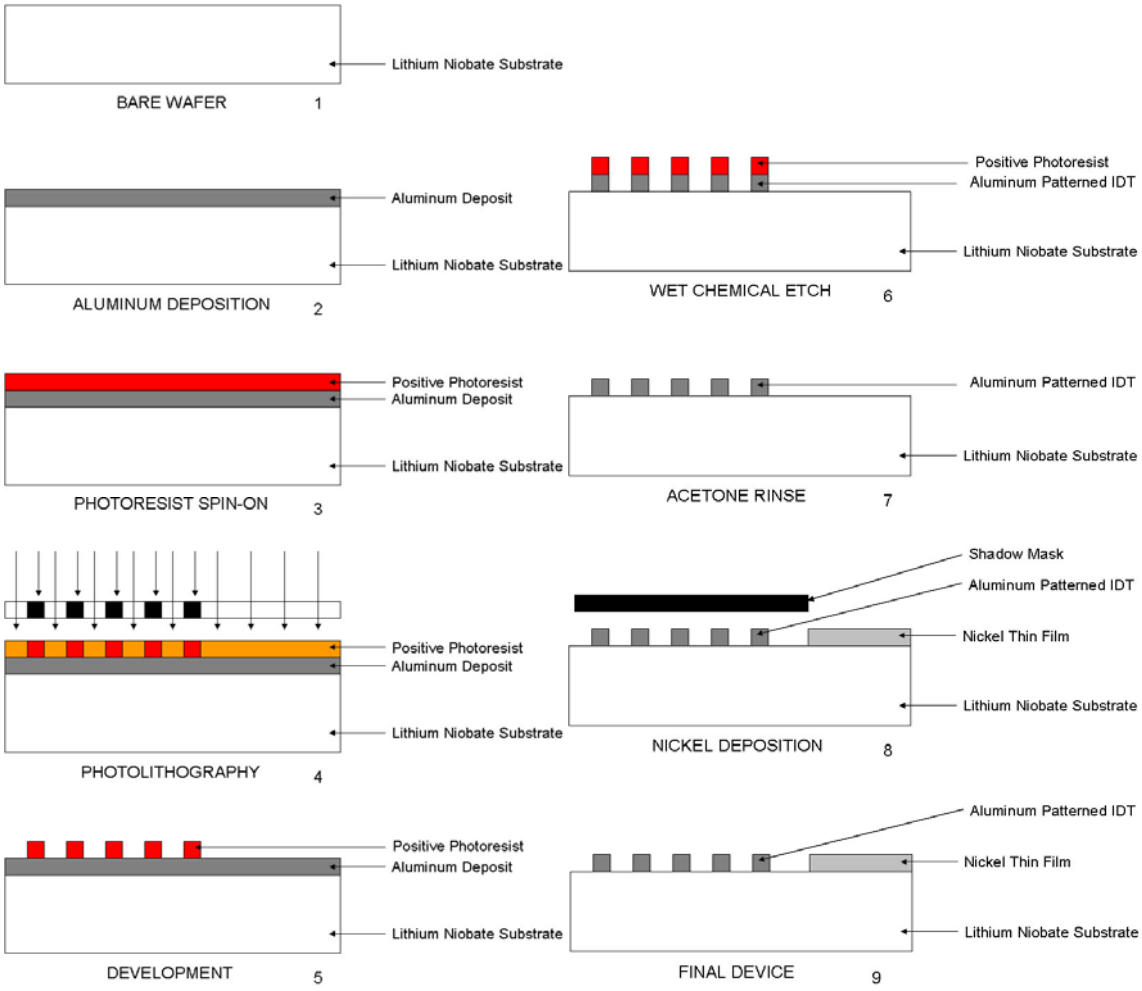

Figure 4 - Process flow for SAW Magnetic Field Sensor. Please note that only the left half of the device is diagramed, and needs to be mirrored along the right vertical axis for complete device diagram.

5.2 AMD/AID Cleaning Procedure

The AMD/AID cleaning procedure is used to remove contaminants and particles from the wafer. This is to ensure that the metal deposits and the photolithography steps do not encounter any manufacturing errors or reduced yields caused by inconsistencies from such particles. AMD stands for Acetone, Methanol, Deionized Water and AID stands for Acetone, Isopropyl Alcohol, Deionized Water.

In both cleaning procedures, acetone is used to douse the wafer for the removal of large particles, organics, and contaminants from the wafer. The wafer is then rinsed in an alcohol (methanol for the AMD cleaning procedure or isopropyl alcohol for the AID cleaning procedure) to remove the acetone residue left behind on the wafer. Finally, the wafer is rinsed with deionized water to remove any trace residue from either the acetone or alcohol. To remove any excess deionized water still present on the wafer, nitrogen gas is blown over the wafer. To dehydrate the wafer further, it is then placed in a soft bake oven at 125°C for at least 10 minutes.

The Oregon State University Device Fabrication Cleanroom originally used the AMD cleaning procedure, but decided to replace the use of methanol with isopropyl alcohol for a number of reasons. Methanol is more expensive than isopropyl alcohol. Methanol also poses a higher health risk to the scientist or engineer handling it. For these two primary reasons, the AID cleaning procedure is now used at Oregon State University in place of the AMD cleaning procedure.

During the first fabrication attempt to manufacture the SAW magnetic field sensor, a 2-inch lithium niobate wafer shattered while being placed in the soft bake oven. After reviewing some manufacturer application notes for lithium niobate, it was determined that lithium niobate has little tolerance for thermal shock [12]. As thermal shock cannot be avoided very well using the bake oven, an alternative cleaning method was performed for the second, third, and fourth fabrication attempts. Instead of using a bake oven to remove the water, high nitrogen flow over the wafer was used instead to remove any remaining water particles, effectively dehydrating the wafer to the extent needed.

5.3 Metal Deposition

There are various metal deposition processes that are commonly used in microelectronic fabrication. The three overarching types metal deposition include evaporation, sputtering and chemical vapor deposition (CVD). Thermal evaporation was used in the creation of the SAW magnetic field sensors due to its simplicity as a process and low cost.

5.3.1 Evaporation

One of the most common and oldest methods for depositing metal onto substrates is through the evaporation process. A wafer is placed on a stand in a sealed chamber, above a metal source, which is then heated to the point of vaporization (usually above the boiling point of the metal). The evaporated metal condenses on the wafer surface leaving a thin film of metal on the wafer. Deposition rates for the evaporation processes can be controlled, but are considered fast compared to other metal deposition processes. A fast aluminum deposit can possess a rate of 6000 Å to 7000 Å per minute [15]. The two primary types of evaporation processes are thermal evaporation and electron-beam evaporation. Thermal evaporation was used for the fabrication of the SAW magnetic field sensors due to tool availability.

In thermal evaporation, the metal source is placed in a boat that is then heated by means of an extremely high current passed through it. The electrical resistance of the boat causes it to heat up to the point where the contents of the boat evaporates. In most cases, the boat is made out of tungsten due to its high melting point (approximately 3410° C) [15]. Metals with boiling points less than 3000° C can make use of this process.

Thermal evaporation takes place under an extremely high vacuum to ensure that contamination levels are minimized and to extend the life of the boats by reducing reacting gases within the chamber.

5.3.2 SAW Magnetic Field Sensor Metal Deposition Details

To create the SAW magnetic field sensor prototype, aluminum and nickel metal depositions were required. The aluminum deposition is done to provide the comb-like alternating electrode structures that make up the interdigital transducers. The nickel deposition places a magnetostrictive thin film in between the interdigital transducers. In both metal depositions, a thermal evaporation process was used as described in Section 5.3.1. A diagram of the thermal evaporation tool setup is shown in Figure 5 below. The procedures followed for depositing the metals are given in the Appendix: Microelectronic Fabrication Tool Procedures.

The Polaron Thermal Evaporation System was used to deposit the aluminum film. A tungsten wire basket was used to hold the aluminum source material and the 2-inch lithium niobate wafer was positioned approximately 8 inches from the aluminum source. The chamber was pumped down to 8×10^{-5} mbar. The boiling point of aluminum as defined in Table 2 is 2792 K. To heat the tungsten wire basket to the point of reaching this temperature, the current passed through the wire basket was raised to 20 A in 5 A increments increased every 5 seconds to allow the basket to slowly adjust to the temperature and current. After approximately 10 seconds of deposition time, the current was raised to 25 A for 5 seconds and then to 30 A for another 5 seconds. The current was

then reduced to 0 A over the course of 10 seconds, allowing for the wire basket to cool down relatively slowly.

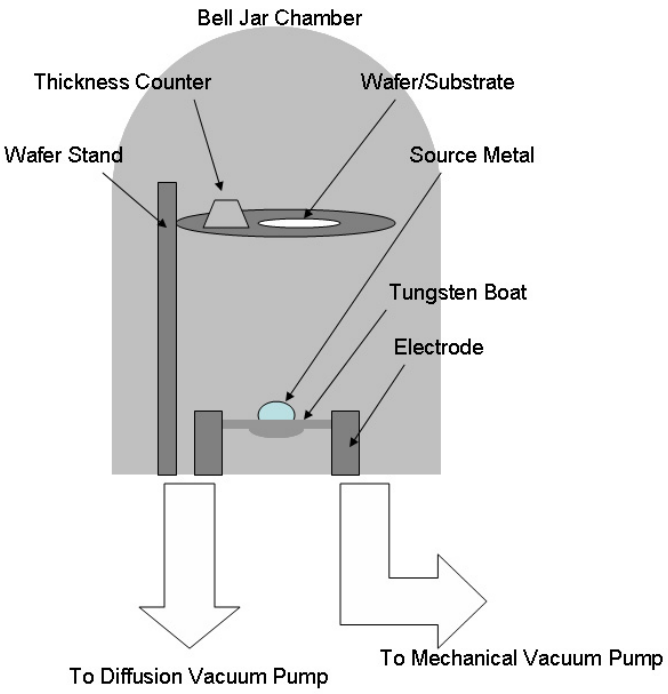

Figure 5 - Chamber diagram of a common thermal evaporator system

This process deposited an aluminum thin film approximately 2000 Å thick as controlled by the amount of aluminum source material supplied. At 2000 Å, enough aluminum is present to keep contact resistance down and ensure that there is a fairly uniform coating. The deposition was completed with no unforeseen issues appearing. The aluminum deposition was performed within specifications, using a standard aluminum source pellet size and standard procedures on the Polaron Thermal Evaporation System.

The nickel film was deposited with the VEECO Thermal Evaporation System. A tungsten boat coated in alumina was used to hold the nickel material. The VEECO

Thermal Evaporation System is used to thermally deposit a variety of different type of metals onto any type of substrate. In contrast, the Polaron Thermal Evaporation System is only used for aluminum depositions. The 2-inch lithium niobate wafer was positioned approximately 8 inches from the nickel source material. A custom shadow mask was created for depositing the nickel metal in between the IDTs of the SAW delay-line devices. Figure 6 depicts an example of a shadow mask used to protect a lithium niobate wafer in areas where the nickel deposits were not wanted.

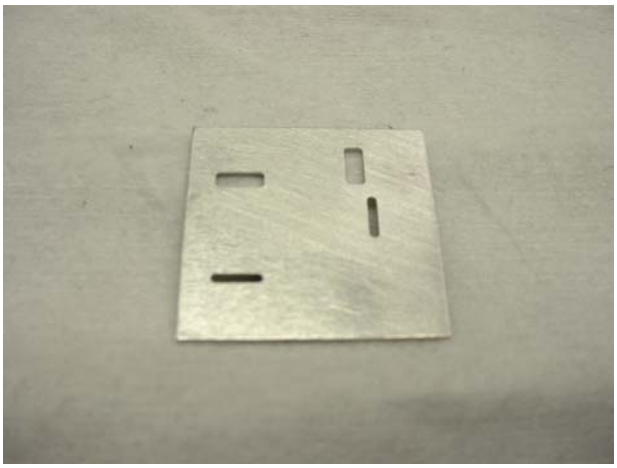

Figure 6 - Picture of a shadow mask used to protect areas of a wafer from metal deposition

The boiling point of nickel metal is 3186 K, which required a maximum current of approximately 200 A to be applied to the tungsten boat. The current was initially ramped up 30 A per minute until 120 A was reached. At this point, a 20 A per minute ramp rate was used until 200 A was approximately reached. A total of 1500 Å was deposited as confirmed on the profilometer, a thickness measuring tool. Issues did arise during the deposition of nickel. For the duration of the process, the chamber possessed a vacuum level of $2x10^{-6}$ torr.

During the first attempts, a 5-mm pellet was used as the nickel source material. This amount was too much, as the required temperature to melt and boil this much nickel exceeded the rated temperature of the tungsten boat. It also caused a phenomenon known as 'wetting' where the excess metal source material melted and spread onto the entire boat, effectively lowering the resistivity of the boat and causing the current to suddenly spike [15, 16]. This phenomenon destroys the boat, which stops the deposition process. This issue was rectified by going to a smaller, 3-mm pellet for the nickel source material. The smaller pellet size took less current to heat up the tungsten boat, and 'wetting' did not occur since the source material was completely contained within the boat's divot.

5.4 Photolithography

Photolithography involves a variety of steps that are used to apply patterns on a wafer. For fabricating SAW delay-line devices, photolithography is used to pattern the interdigital transducers out of the aluminum layer put down during the thermal evaporation process.

5.4.1 Photoresist

In the first step, a layer of photoresist is spun onto the wafer on top of the material layers that were previously deposited or grown onto the wafer. This light-sensitive material is used as a barrier material to protect the wafer and its material layers from the next process; namely wet chemical etching. There are two types of photoresist. Positive photoresist possesses a chemical structure, in which its bonds are substantially weakened

when exposed to ultraviolet light. Negative photoresist possesses a chemical structure, in which its bonds are strengthened when exposed to ultraviolet light. Positive photoresist has become the industry standard due to its better process control for small structures. Usually, the photoresist is baked onto the wafer at temperatures around 115°C for 60 seconds to harden and stabilize the barrier material, and to evaporate the solvent present in the photoresist (the solvent is what gives photoresist its viscosity).

5.4.2 Photomask Alignment and UV Light Exposure

To apply the appropriate pattern, a photomask with the desired pattern is placed on top of the newly photoresist-coated wafer. A photomask can be made out of either chrome or Mylar. A Mylar photomask was used to fabricate the SAW magnetic field sensors for this project. The mask used for the patterning of the SAW magnetic field sensor is shown in Figure 7. An aligner exposes the wafer high-intensity ultraviolet (UV) light where the photomask was transparent. The photoresist chemically reacts to the UV light, either weakening or strengthening depending on the type of photoresist used. A developer solution is used to remove the weakened or non-strengthened photoresist, exposing the layers underneath the photoresist.

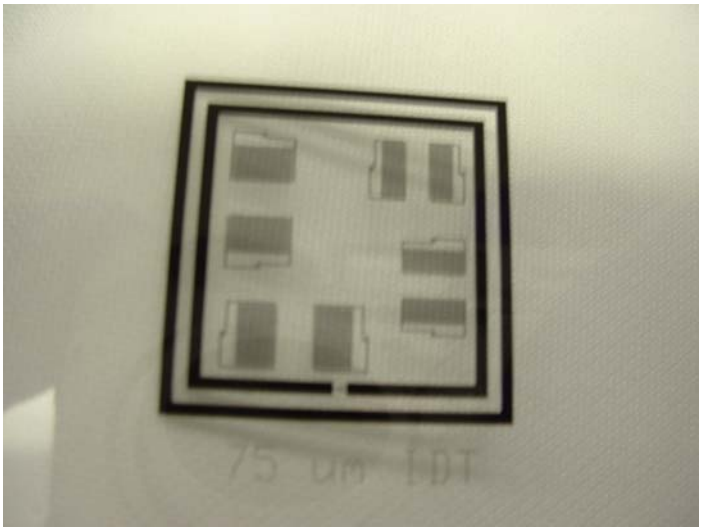

Figure 7 - Picture of a 75-micron photomask used to pattern the IDTs onto lithium niobate substrates

5.4.3 SAW Magnetic Field Sensor Photolithography Details

In the manufacturing of the SAW magnetic field sensor, 20 drops of positive-type photoresist was spun on at 3000 rpm for 10 seconds, and then ramped up to 4000 rpm for 20 seconds. This was followed by a soft bake to evaporate the solvent in the photoresist and to harden the mask. The soft bake was performed on a hot plate set to 85°C and was left on it for 10 minutes. It should be noted that issues potentially arose when performing the soft bake. During the second attempt to fabricate the SAW magnetic field sensor, a fracture that spanned the entire wafer along the y-axis appeared. Lithium niobate is reportedly prone to thermal shock, as found out in Section 5.2. The lithium niobate wafer was placed onto the hot plate after approximately 5 seconds of adjustment time. It is suspected that the fracture was caused by thermal shock stresses during the placement of the wafer onto the hot plate. Since the fracture was discovered only after the completion of UV exposure on the aligner, the cause of the fracture remains speculation. Adjustments to the soft bake procedures were made, with a slower 10 second wafer

introduction to the hot plate. The third and fourth fabrication attempts did not break or fracture the wafer using this new procedure.

The photomask used was patterned with various SAW interdigital transducer designs to be laid out in aluminum. The minimum feature size on the photomask was 25 microns. The design was created by the Oregon State University Chemistry department. A Karl Seuss MJB3 Aligner was used to expose the wafer to the UV light for a 10 second period of time. Commercial-grade developer solution was used to remove the exposed photoresist. The sample was agitated in the developer solution for 30 seconds. Issues arose using the 25-micron feature size photomask during the second and third attempts. The IDT patterns were prone to blemishes, line breaks, and poor development in general. To rectify the problem, a photomask possessing interdigital transducer designs that had 75-micron feature sizes was used instead of the 25-micron feature size photomask. The fourth attempt was successful using the new photomask. The IDT patterns were clean and of high quality in general. At this point, the lithium niobate wafer possessed a uniform layer of aluminum on its front surface with the area outlining the transducer pattern covered in a layer of photoresist.

5.5 Metal Wet Etch

The etch process is used for the removal of an unwanted material layer that is not protected by photoresist. This process is used for patterning wafers after photolithography, or it is used for cleaning wafers by removing an entire material layer indiscriminately. There are two types of etching techniques: dry etching and wet etching. Figure 8 shows the etching profiles of the two types of etching techniques. For the

fabrication of the SAW magnetic field sensors, a wet etch technique was selected for tool availability reasons.

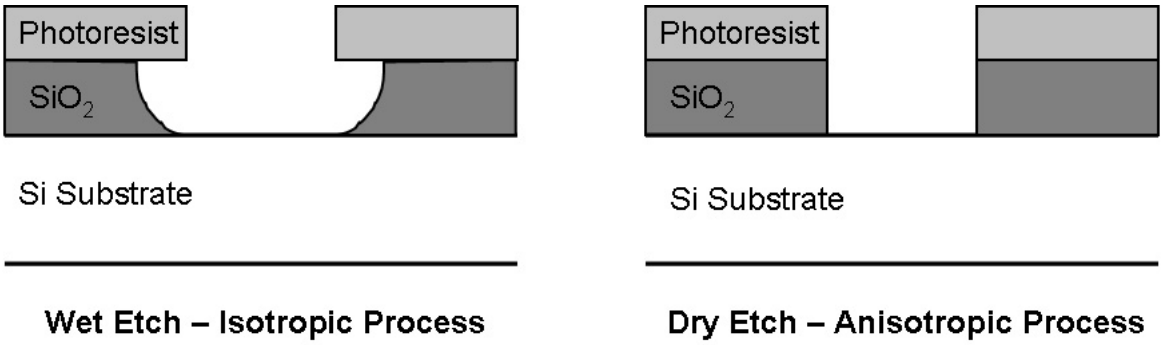

Figure 8 - Profiles of wet etch and dry etch processes

5.5.1 Wet Etching

The wet chemical etch process involves placing the wafer into an acid bath, which selectively removes a particular material layer depending on what type of acid solution is used. Some of the common material layers that are etched off using a wet chemical etch process include silicon dioxide, which is etched off with hydrofluoric acid (HF), and metal layers such as aluminum, which is etched off with an acid solution made up of predominantly phosphoric acid (H_3PO_4) [16]. The acid solutions do not etch through the photoresist barrier layer, protecting the material layer beneath it to an extent. Wet chemical etching is an isotropic process, etching the targeted material layer in all directions equally. There is a potential for over-etching underneath the photoresist barrier if the wafer is left in the acid bath for too long. Once the material layer not protected by the photoresist barrier is removed, leaving only the desired pattern, the

photoresist is removed by dousing the wafer with acetone, followed by an AMD or AID clean.

5.5.2 SAW Magnetic Field Sensor Etching Details

For the fabrication of the SAW magnetic field sensor samples, a chemical wet etch process was used to remove the unwanted aluminum to expose the interdigital transducer patterns. The wet etch process was selected over the dry etch process due to the lack of tool availability and training, along with the fact that wet etch processes are easier to carry out and are faster to perform. The acid bath solution developed to remove the aluminum possessed the following chemical ratios:

Chemical	***Formula***	***Ratio***	***Actual Amount***
Phosphoric Acid	H_3PO_4	80%	80 mL
Deionized Water	H_2O, 16 MΩ	10%	10 mL
Nitric Acid	HNO_3	5%	5 mL
Acetic Acid	CH_3COOH	5%	5 mL

Table 4: Acid Bath Solution Composition

The wafer was placed in the acid bath for 1 minute and 20 seconds with an acid solution uniform temperature of 50°C (heated on a hot plate). The wafer was promptly removed from the acid solution and rinsed with deionized water once all of the aluminum not protected by the photoresist was visibly etched away.

At this point the wafer was cleaned, removing the photoresist protective layer with acetone. The wafer went through an AMD cleaning process before being prepared for the nickel metal deposition step. Please refer to Section 5.2 and Section 5.3 for information on the AMD cleaning process and the nickel deposition process respectively.

6. Applications and Sensor Comparison

The SAW magnetic field sensor has many potential applications including field position sensing, proximity detection, magnetic field detection, structural health monitors, and industrial control systems [17]. SAW magnetic field sensors could potentially be used for position and proximity detection through the use of an array of sensors. Each sensor in the array could potentially determine the distance of a magnetized object (to supply the external magnetic field) from the sensor. With multiple sensors determining the distance of this object from them, the position of the device can be then triangulated as long as the locations of the SAW magnetic field sensors are static relative to each other. A potential set-up for a structural health monitor would involve a similar system, where these SAW magnetic sensors could be deployed on iron or steel beams within buildings or on the hull of an aircraft or spacecraft [17]. As the steel or ferromagnetic material bends due to stress, the localized magnetic field changes a minute amount, but enough to be detected by the SAW magnetic field sensor, alerting that a potential buckle in the material might occur. There are numerous ways that SAW magnetic field sensors could potentially be deployed.

With the increasing need for monitoring systems, a SAW magnetic field sensor could potentially complement the sensors currently available for these applications. There are some major potential advantages associated with deploying SAW magnetic field sensors over sensors currently on the market, but before these advantages are to be described, a basic explanation of how some common, currently available sensors work is in order. The most common techniques for detecting magnetic field make use of the Hall Effect or magnetoresistive materials.

6.1 Hall Effect Sensors

Hall Effect sensors are capable of detecting both the direction and the intensity of magnetic fields [18]. Most Hall Effect sensors are composed of a conducting plate with contacts on opposite sides of the plate flowing current through the plate. A magnetic field that is normal to the surface of the metal plate is the component that will affect the detection. On the sides of the conducting plate perpendicular to the current contact sides, a high voltage known as the Hall voltage can be detected. This voltage is given by equation 3 [3, 4, 18].

$$V_H = R_H \frac{IB_{normal}}{thx} \qquad \text{(Equation 3)}$$

In equation 3, 'V_H' is the Hall voltage, 'R_H' is the Hall coefficient associated with the conducting plate material, 'I' is the current flowing across the conducting plate, 'thx' is the thickness of the conducting plate, and 'B_{normal}' is the magnetic field component that is normal to the conducting plate surface. A depiction of a basic Hall sensor is shown in Figure 9 [3, 4]. Another common configuration for Hall Effect sensors makes use of a full bridge, with equal resistors on three of the four sides and an offset resistor on the fourth side. An excitation voltage is applied to one of the four corners while the opposite corner is shunted to ground. The voltage outputs from the other two corners are then compared to measure the change [18].

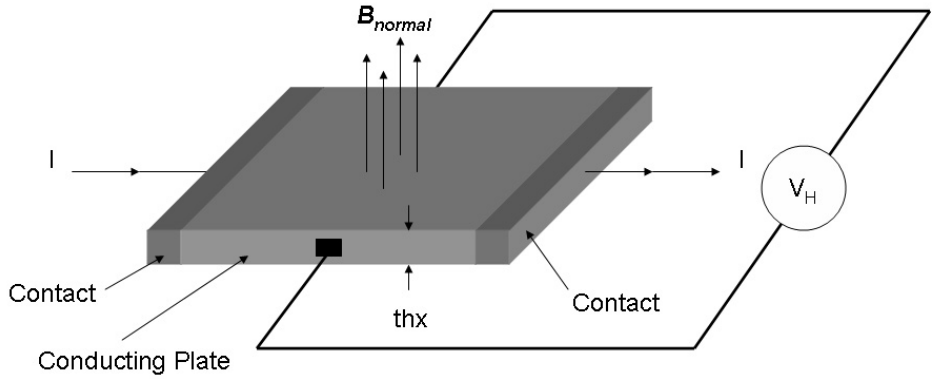

Figure 9 - Depiction of a basic plate Hall sensor

In general, Hall Effect sensors have a detection range on the order of mT (milli-teslas) [3, 4]. They are very low cost, and have a sensitivity range of around 5 to 500 mV/mT [3] where the typical sensitivity is around 50 mV/mT [4]. They can be manufactured using standard microelectronic fabrication processes as well.

6.2 Magnetoresistive Sensors

Many of the magnetic sensors on the market today make use of the magnetoresistive effect. Magnetoresistivity involves a change in resistivity of a current-carrying magnetic material caused by the presence of an external magnetic field [4, 11, 18]. For most conductive materials, their resistance will increase in the presence of a magnetic field. The primary cause of magnetoresistivity is the Lorentz force [3, 18], which causes electrons to move in curved paths resulting in increased electron collisions, thus an increase in resistivity. Both anisotropic magnetoresistors (AMR) and giant magnetoresistors (GMR) are used as magnetic sensors.

AMR-based devices are usually made out of a single-layer magnetic thin film such as Permalloy (most AMR thin films are based on a Ni-Fe combination) [4, 11]. The

AMR effect is based upon the fact that the magnetic thin film has increased resistance when the external magnetic field is parallel to the current flowing through the magnetic thin film. There is approximately a maximum change of 2% to 3% resistance that occurs due to an external magnetic field [4, 18].

The GMR effect occurs when a conductive, non-magnetic thin film is sandwiched in between two conductive, magnetic thin films. A current is applied normal to the thin film layers. When an external magnetic field is applied, the top magnetic thin film layer's magnetization is affected and changes depending on the external field [4, 18]. Depending on the magnetization directions in the two outer magnetic thin film layers, the resistance will change. When the two films possess magnetizations going in the same directions, the resistance is substantially less than the resistance generated when the two films possess magnetizations in the opposite directions. This is depicted in Figure 10.

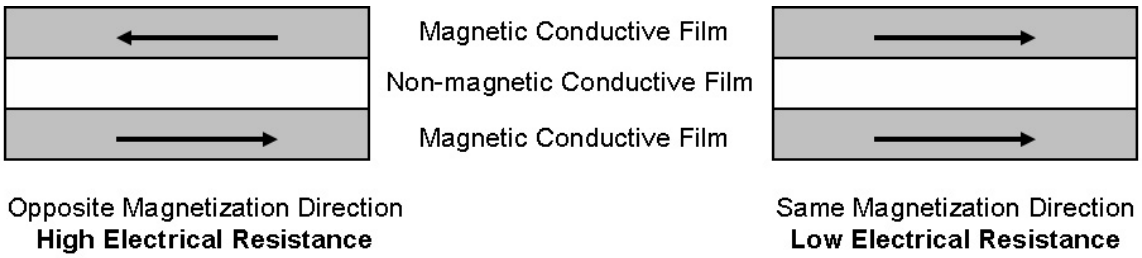

Figure 10 - GMR Effect: Resistance is dependent on the relative magnetization directions of the two magnetic thin film layers

6.3 Magnetic Field Sensor Comparison

As a point of comparison between a few of the currently available sensor types used for detecting magnetic fields, Table 5 provides some general characteristics of each

type of sensor [4]. Table 6 provides theoretical literature information for the SAW magnetic field sensor [2, 3, 9, 11]

Parameter	***AMR Sensor***	***GMR Sensor***	***Hall Effect Sensor***
Input Range	25 mT	2 mT	60 mT
Max Output/Sensitivity	2% to 5% change	4% to 20% change	0.5 V/T
Frequency Range	Up to 50 MHz	Up to 100 MHz	25 kHz typical
Temperature Coefficient	Fair	Good	Depends on model
Maximal Temperature	200°C	200°C	150°C
Cost (as of 2000)	Medium to high	Low to medium	Low

Table 5 - General characteristics of common magnetic field sensors

Parameter	***SAW Magnetic Field Sensor***	***Source***
Input Range	1-100 μT up to 1-100 mT	[3]
Max Output/Sensitivity	1 Hz/μT	[3]
Frequency Range	30 MHz to 500 MHz, nominal @ 210 MHz	[2], [9]
Temperature Coefficient	Poor to Fair (94 ppm/°C)	[2]
Maximal Temperature	200°C (Based off of nickel properties)	[11]
Cost	High	[3]

Table 6 - SAW Magnetic Field Sensor Characteristics

The primary advantage that SAW magnetic field sensors have over current sensor technologies is its extremely high sensitivity. In addition to the high sensitivity level, recent advances in wireless SAW interrogation provides a benefit that none of the other sensors can provide [7, 18, 19]. The SAW magnetic field sensor could easily be modified to accommodate wireless transmission and reception. A radio frequency (RF) antenna would be attached to one of the IDTs, while the other IDT would be converted into a reflector. The IDT with the RF antenna would receive an RF signal, converting it into a mechanical surface wave and launching it across the surface of the substrate towards the reflector. The surface wave would then be affected by the measurand across the length of the SAW device before reaching the reflector. The reflector would then bounce the wave

back towards the IDT, where the surface wave would once again be affected by the measurand, effectively doubling the effects of the measurand on the surface wave. Once the surface wave returned to the IDT, the surface wave would then be converted back into an RF signal. With the ability to receive and transmit radio frequency (RF) signals, SAW magnetic field sensors can be positioned in extreme environments [7]. SAW devices in general are quite rugged requiring little to no servicing, and the SAW magnetic field sensor design is no exception. In addition to the advantages of being wirelessly interrogated, SAW magnetic field sensors have the potential to be completely passive, meaning that they do not need to be powered. A wireless interrogation unit for transmitting and receiving signals from the passive SAW magnetic field sensor would provide the sensor with the radio frequency (RF) pulse needed to determine the magnetic field [7, 18, 19]. All of the common magnetic sensors in use today are active sensors, requiring power to detect changes in magnetic field. This has major implications in cost and power savings.

7. Fabrication Results and Conclusions

A fully processed surface acoustic wave magnetic field sensor device was completed after four attempts due to various difficulties and issues that had to be overcome. In the end, the fabrication process flow used was successful in generating devices. At each step in the process flow, the device was inspected for process defects, blemishes and breaks in the thin films. By the fourth attempt, no critical damage or defect was apparent on the lithium niobate piezoelectric substrate or in the thin films.

The final SAW magnetic field sensor device fabricated was based on a 2-inch, Y-cut (waves propagating in Z-direction) lithium niobate wafer (piezoelectric substrate). The IDTs were fabricated out of aluminum and patterned using standard photolithography processes. The SAW devices are shown in Figure 11. A nickel thin film was applied through a shadow mask during a thermal evaporation process to put down the stimulus-reacting component of the sensor. These device dimensions were set by the photolithography masks used to create the SAW devices based on a design by the Oregon State University Chemistry Department. Table 7 details additional parameters about the interdigital transducers, such as the number of electrode "fingers" on each IDT, the distance between IDTs, the width of the IDTs, and connecting channel width of the IDTs. Figure 12 provides a diagram of the IDTs with appropriate labels to complement Table 7 while Figures 13 and 14 provide microscope pictures of the actual fabricated IDTs with measurements of the IDT channel width and IDT finger width.

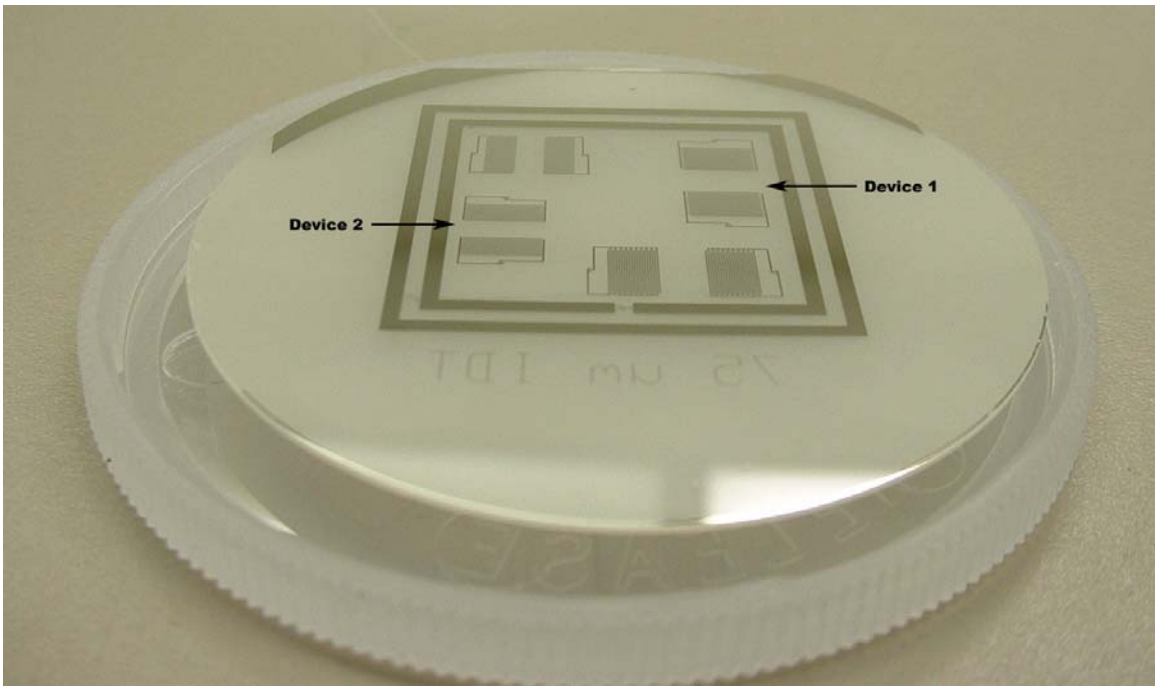

Figure 11 - Picture of fabricated SAW devices

Device 1	***Value***	***Device 2***	***Value***
# of 'fingers' per electrode	10	# of 'fingers' per electrode	10
# of 'fingers' per IDT	20	# of 'fingers' per IDT	20
'Finger' width (w_f)	76 μm	'Finger' width	60 μm
Spacing width (w_s)	75 μm	Spacing width (w_s)	60 μm
'Finger' period length (d)	302 μm	'Finger' period length (d)	240 μm
Distance between IDTs (l_s)	~3 mm	Distance between IDTs (s)	~2 mm
Distance between IDT centers (l)	~6 mm	Distance between IDT centers (l)	~4 mm
IDT total width (w)	~3 mm	IDT total width (w)	~2 mm
IDT total length (h)	5 mm	IDT total length (h)	5 mm
IDT channel width (w_{ch})	93 μm	IDT channel width (w_{ch})	93 μm
Thin film clearance from IDTs on either side (l_m)	~1 mm	Thin film clearance from IDTs on either side	~0.5 mm
Width of the magnetic thin film (w_m)	~1 mm	Width of the magnetic thin film (w_m)	~1 mm

Table 7 - Interdigital transducer parameters of fabricated device

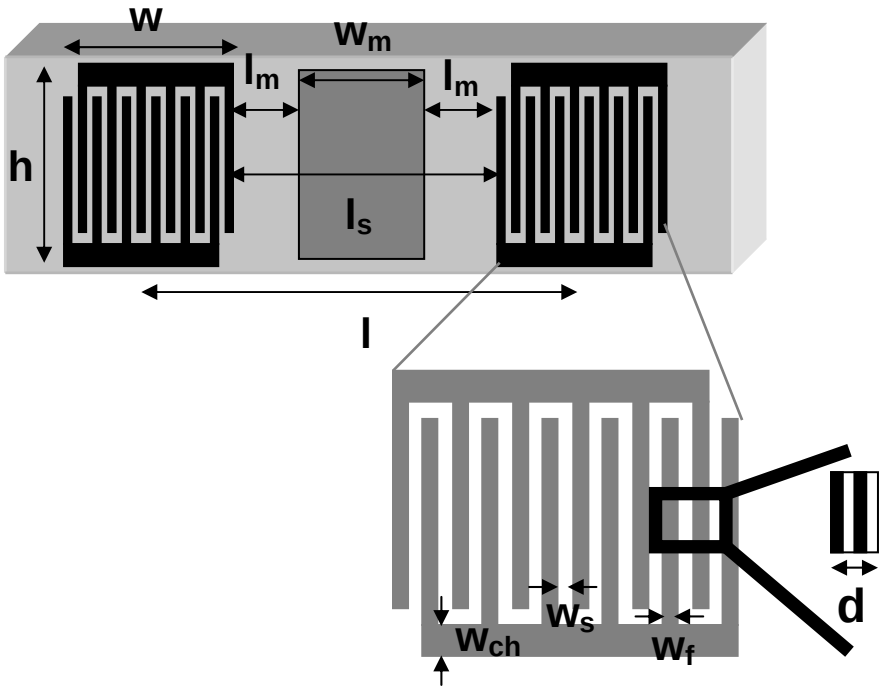

Figure 12 - Labeled diagram of interdigital transducer

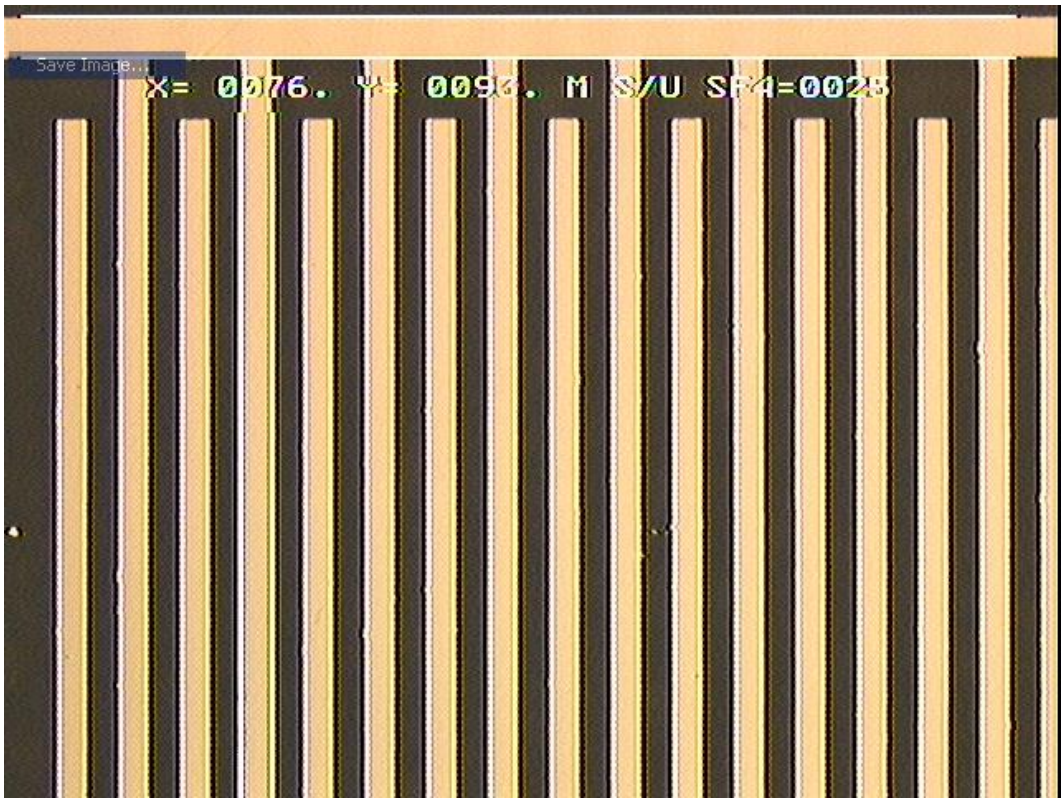

Figure 13 - Microscope picture at 100x displaying fabricated IDTs on Device 1 (as defined in Figure 11) with an IDT channel width of 93 microns (Y= 0093) and an IDT finger width of 76 microns (X= 0076)

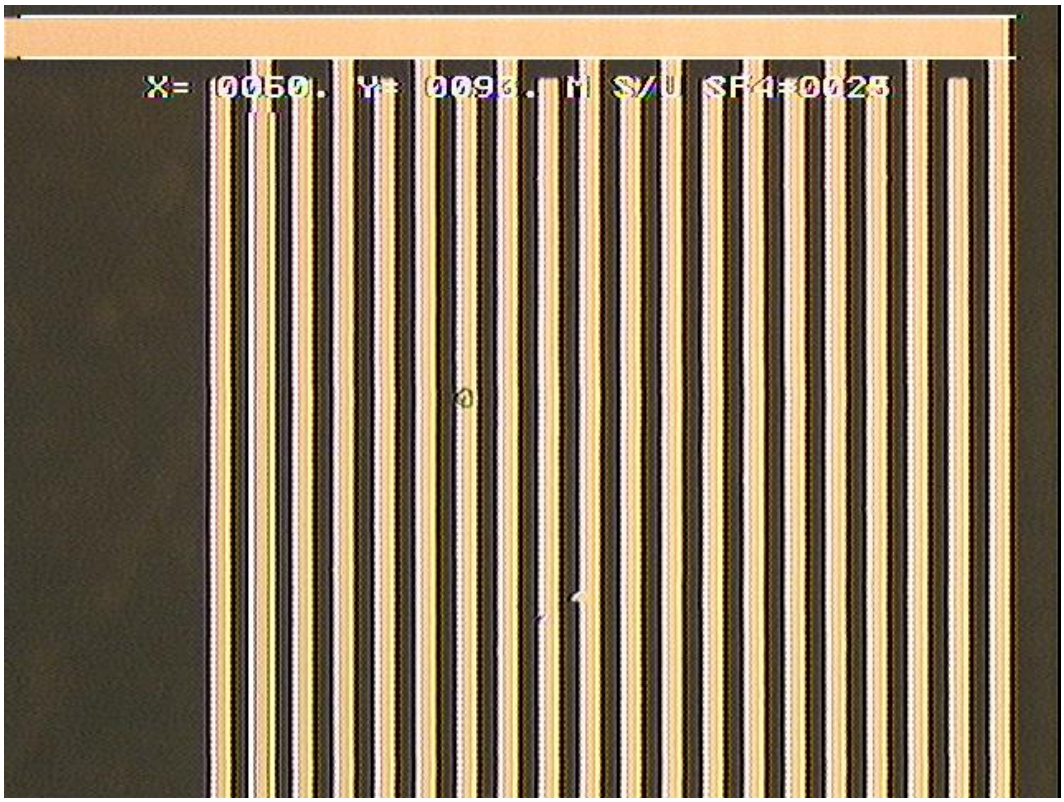

Figure 14 - Microscope picture at 100x displaying fabricated IDTs on Device 2 (as defined in Figure 11) with an IDT channel width of 93 microns (Y= 0093) and an IDT finger width of 60 microns (X= 0060)

As can be seen from Figure 11 and from Figures 13 and 14, two SAW magnetic field sensor devices were produced with different finger widths and spacing widths. Since the synchronous frequencies and time delay are both dependent upon the spacing and finger widths if the distance between the IDTs are kept constant, the two devices will have different optimal operating frequencies and potentially different time delay base points. These differences though should not affect either of the device's ability to detect magnetic fields as long as each one has an input voltage specifically optimized for that particular device.

Not taking the magnetic thin film into account, the optimal or synchronous frequency that would work best for the fabricated Device 1 SAW delay-line would be

11.55 MHz calculated from Equation 1 from Section 3.1 using the Table 1 to find the wave velocity in lithium niobate (v_0 = 3488 m/s) and using Table 7 for the finger periodicity (d = 302 microns). The time delay associated with the fabricated Device 2 SAW delay-line neglecting the effects of the magnetic thin film should be approximately 1.72 μs calculated from Equation 2 from Section 3.1, using Table 7 to find the distance between the IDT centers (l = 6 mm) and using Table 1 to find the wave velocity for lithium niobate (v_0 = 3488 m/s). The theoretical values of synchronous frequency and timed delay for Device 2 can be solved with the same equations and tables used to solve for the values of Device 1. The synchronous frequency of Device 2 theoretically should be 14.53 MHz (v_0 = 3488 m/s and d = 240 microns). The time delay between the transmission and the receiving of the surface wave across Device 2 theoretically should be 1.15 μs (l = 4 mm and v_0 = 3488 m/s).

With the presence of the magnetic thin film and a magnetic field, the time delay will be affected. An increase in time delay should occur with the addition of the magnetic thin film in between the two IDTs, and a further increase in time delay should be seen with the presence of an externally applied magnetic field. This is caused by a decrease in the surface wave velocity in the lithium niobate [20]. The strain in the crystal lattice structure of the lithium niobate due to the length change in the magnetostrictive thin film reduces the velocity in which waves can propagate through the crystal. Quantitative evidence that the SAW magnetic field sensor will operate in such a manner is not available as it is outside the scope of this study, but should be considered for a future continuation to this study.

Although this study strictly focused on a theoretical review of a SAW-based magnetic field sensor and a method of fabricating such a device, there are many areas for continued study in this subject matter. The characterization of the fabricated device is the most probable next step, which can be accomplished using a network analyzer system and probe station. Research into signal conditioning for this particular sensor is another area of research that could be pursued, in attempts to increase the signal-to-noise output and reduce the effects of interference.

Bibliography

[1] David P. Morgan, " History of SAW Devices," Proceedings of the 1998 IEEE International Frequency Control Symposium, 1998., pp. 439-460, 27-29 May, 1998.

[2] Bill Drafts, "Acoustic Wave Technology Sensors," IEEE Transactions on Microwave Theory and Techniques, vol. 49, no. 4, pp. 795-802, April 2001.

[3] Julian W. Gardner, Vijay K. Varadan, Osama O. Awadelkarim, Microsensors, MEMS and Smart Devices, First ed. , New York, New York: John Wiley and Sons, LTD, 2001.

[4] Ramon Pallas-Areny and John G. Webster, Sensors and Signal Conditioning, Second ed., New York, New York: John Wiley and Sons, LTD, 2001.

[5] D. S. Ballantine, R. M. White, S. J. Martin, A. J. Ricco, E. T. Zellers, G. C. Frye, H. Wohltjen, Acoustic Wave Sensors, First ed. , Chestnut Hill, MA, USA: Academic Press, 1997.

[6] Ewald Benes, Martin Groschl, Granz Seifert, Alfred Pohl, " Comparison Between BAW and SAW Sensor Principles," IEEE Transactions on Ultrasonics, Ferroelectrics, and Frequency Control, vol. 45, no. 5, pp. 1314-1330, September 1998.

[7] Ulrich Wolff, Franz Ludwig Dickert, Gerhard K. Fischeraurer, Wolfgang Greibl, Clemens C. Ruppel, " SAW Sensors for Harsh Environments," IEEE Sensors Journal, vol. 1, no. 1, pp. 4-13, June 2001.

[8] C.A. Johnsen, T.L. Bagwell, J.L. Henderson, R.C. Bray, “Polyimide as an Acoustic Absorber for High Frequency SAW Applications," IEEE 1988 Ultrasonics Symposium Proceedings, 1988., pp. 279-284, 2-5 October 1988.

[9] William P. Robbins, Alex Hietala, " A Simple Phenomenological Model of Tunable SAW Devices Using Magnetostrictive Thin Films," IEEE Transactions on Ultrasonics, Ferroelectrics, and Frequency Control, vol. 35, no. 6, pp. 718-722, November 1988.

[10] Samy M. Hanna, " Magnetic Field Sensors Based on SAW Propagation in Magnetic Films," IEEE Transactions on Ultrasonics, Ferroelectrics, and Frequency Control, vol. 34, no. 2, pp. 191-194, March 1987.

[11] Richard M. Bozorth, Ferromagnetism, First reissued ed., Piscataway, NJ: IEEE Press, 1951, reissued 1993.

[12] Crystal Technology, Inc., Lithium Niobate: Application Notes, First ed., Palo Alto, CA: EPCOS Company, 2001.

[13] G. Dewey and S. Datta. Private Communication, 2005.

[14] Richard C. Jaeger, Volume V: Introduction to Microelectronic Fabrication, Second ed., Upper Saddle River, NJ: Prentice Hall, 2002.

[15] H. Chiang and R. Presley. Private Communication, 2006.

[16] T. K. Plant. Private Communication, 2006.

[17] Jacob Fraden, Handbook of Modern Sensors, Second ed., Woodbury, NY: American Institute of Physics Press, 1997.

[18] P. Dhagat and A. Jander. Private Communication, 2006.

[19] Alfred Pohl, " A Review of Wireless SAW Sensors," IEEE Transactions on Ultrasonics, Ferroelectrics, and Frequency Control, vol. 47, no. 2, pp. 317-332, March 2000.

[20] Jeong-Sik Choi, Jong-Dae Moon, Cheol-Ho So, Cha, In Su, " A Study on Properties of SAW and the Magnetic Thin-Film Bond," IEEE 4th Conference on Vacuum Electronics Proceedings, 2003., pp. 179-180, 28-30 May 2003.

Appendix: Microelectronic Fabrication Tool Procedures

THE POLARON EVAPORATION SYSTEM OPERATION MANUAL

Department of Electrical and Computer Engineering
Oregon State University

1 HISTORY

Date	Name	Changes
Nov. 18, 2002	Jeff Bender	Document Created
Jan. 30, 2002	Jeff Bender	4 Added reorder information for W baskets.

2 INTRODUCTION

The system is essentially a smaller desktop version of the Veeco thermal evaporation system. Like the Veeco, the system consists of a diffusion pump for the creation of a high vacuum, a mechanical pump which both backs the foreline of the diffusion pump and roughs the chamber from atmosphere to crossover, and a bell jar containing electrodes for thermal evaporation of material using resistive heating.

Unlike the Veeco, there is no cold trap on the diffusion pump, the ultimate pressure is significantly higher, only one thermal source is present in the system, a thickness monitor is not employed, and operation of the systems is completely manual (i.e. no valve actuation and interlocking). Chamber pressure is monitored using capacitance manometer and cold-cathode Penning gauges instead of thermocouple and B-A ionization gauges.

Additionally, **the Polaron evaporation system is only to be used to deposit metallization**. All other materials should be done using the Veeco. Normally the system is configured to evaporate Al from a W wire basket; talk with a system reference before using other metals or changing the electrode configuration.

3 EVAPORATION PROCEDURE

All operators must be thoroughly checked out on the use of this machine by trained personnel before operating equipment!

3.1 Loading substrates

1. Before starting, make sure that the mechanical and diffusion pumps have been working at least for 1 hour. Since the power to the system and all components is hard-wired this should always be the case, excepting power failures.

2. Be sure that the system is in its standby conditions: the high vacuum valve should be closed and the mechanical pump valve should be set to backing.

3. Remove the implosion guard and vent the chamber by turning the vent valve counter-clockwise to bleed N_2 into the chamber, holding the bell jar lightly in place. Tighten the valve finger tight when atmosphere is reached.

4. Remove the bell jar by slowly and carefully lifting it, being careful not to damage the rubber seal on the bottom. Place the bell jar on a firm, clean surface where it can not be accidentally pushed onto the floor.

5. Remove the cylindrical Al shield, exposing the electrodes and W filament source basket.

6. Use tweezers to extract an Al clip from the jar of clips and place it in the bottom of the W basket, "V" down.

7. Carefully replace the Al shield, taking care the the shield is situated so that the shutter can be opened.

8. Using glass slides and/or shadow masks, situate your substrate(s) as nearly directly above the W basket as possible. Since the mechanical pump is integrated into the unit, vibrations often move the substrates during the run. To minimize this effect, place a clear piece of glass over your substrate and weight it down with the two metal weights found in the chamber.

   Note: two sets of masks for round Al dots are always located near the system. The Planar masks (with smaller dots down the middle) produces dots with areas of 0.085 cm^2, while the other mask produces dots with areas of 0.079 cm^2.

9. Carefully replace the bell jar, taking care not to scuff the rubber seal and that the shutter has clearance to open.

10. Move the mechanical pump valve from "backing" to "roughing" and wait several minutes for the pressure shown on the cap man gauge to drop to about 1 Pa.

11. Return the system to "backing" and watch the cap man gauge, which now reads foreline pressure. This pressure will be fairly high after roughing due to leakage. Wait until the foreline pressure has recovered before continuing.

12. Open the high vac valve and wait roughly 20 minutes. Turn on the Penning gauge and wait until 10^{-4} is reached. Evaporation above this pressure will result in the deposition of aluminum oxide instead of aluminum.

3.2 Evaporation

1. Begin by turning on the evaporation source; the system will not allow the supply to be turned on unless the vacuum level is sufficiently high, indicated by an orange light.

2. To the left of the power switch is the evaporation control. Select "continuous" with the toggle switch.

3. Slowly increase the current control knob. The filament will begin to glow. Open the shutter and look through the bell jar down on the glass substrate.

4. Continue slowly increasing the current until the Al clip melts. Pause, then slowly increase the current again. The Al will evaporate, and a film will begin to be deposited on the substrate. The current will be around 20 A.

5. When the basket cannot be seen any longer and the room lights are reflected by the deposited Al, close the shutter. The deposited thickness of Al is 150-200 nm.

6. Increase the current further by about 5 A. Wait several seconds to ensure that all Al is evaporated from the wire basket.

   FAILURE TO DO THIS SEVERELY LIMITS THE LIFE OF THE W BASKET!!!

7. Decrease the current to zero, place the evaporation control rocker switch in the neutral position, and turn off the evaporation source and the Penning gauge.

8. Wait ~5 min for the system to cool down; this will also dramatically improve the lifetime of the W basket.

9. Close the high vac valve.

3.3 Shutdown

1. Vent the chamber as described in Sec. 3.1.

2. Remove your substrate(s) and replace the bell jar carefully.

3. Rotate the valve actuator to "roughing" and wait until the crossover pressure is reached.

4. Rotate the valve actuator to "backing;" the system is now in its standby mode.

4 Changing Baskets

The W basket will need to be changed occasionally (after > 100 evaporations, or far sooner if it has been inappropriately abused). Changing the basket is easy: just loosen the hex screws holding the old wire in place, slide in a new basket (look in "Evaporation Supplies" in the supply room), and retighten the screws. Be very careful to avoid overtightening, however: remember that these electrodes will become very hot and expand. Slightly past finger tight is sufficient.

New baskets should be ordered when the supply begins running low. W baskets can be bought from the R. D. Mathis company (562-426-7049). Order part number "ME 17 - 3x.025W".

THE VEECO EVAPORATION SYSTEM OPERATION MANUAL

Department of Electrical and Computer Engineering
Oregon State University

1 HISTORY

Date	Name	Changes
1989	John Ebner, Hyungmo Yoo, Tagore Kollipara, and Leon Ungier	Document created.
July 4, 2001	Jeff Bender	Revised to reflect current system state and procedure.
Nov. 17, 2002	Jeff Bender	Comments regarding venting and contamination.

2 INTRODUCTION

The system can be divided into five basic sections: a diffusion pump system, a mechanical pump, a chamber consisting of a bell jar and hoist, system controls, and cabinetry.

The diffusion pump system consists of a 4-stage oil diffusion pump, a water-cooled baffle/cold combination, a liquid nitrogen tank for pumping of condensable vapors, a high vacuum valve, a baseplate onto which the vacuum chamber is mounted, and the manifolding required to valve the mechanical pump between the foreline of the diffusion pump and the chamber roughing valve. The manifold also includes thermocouple gauges which are used to monitor foreline and roughing pressures, a leak test quick coupling, and a vent valve. The mechanical pump is used to evacuate the chamber from atmospheric pressure to a level at which the diffusion pump can be utilized.

The system controls consist of a single lever valve control, two stations thermocouple gauge, and an ionization gauge control. The control panel includes circuit breakers for the mechanical and diffusion pumps, readouts for the roughing and foreline thermocouple gauges, a vacuum system logic schematic with lights that indicate valve positions, and a single-lever valve control with adequate interlocks and time delays to assure proper sequencing.

The ionization gauge control is connected to a Bayard-Alpert type ionization gauge tube that can be mounted in quick couplings either in the chamber or below the high vacuum valve.

The evaporation power supply is located at the right of the guage controls and is used to proved and monitor evaporation current to selected current feedthroughs. These are located at the bottom left front of the unit. A current cord is attached to the hole whose numbers correspond to the boats inside the chamber, numbered from left to right. The power supply voltage is selected by rotated the Variac dial; current is read out on the guage.

The bell jar hoist is a manual counterbalanced type. The counterweight is within the support mast and is connected by a steel cable via pulleys to the top of the bell jar. The bell jar is guided by two guide rods and is self-aligning with the base plate.

3 EVAPORATION PROCEDURE

All operators must be thoroughly checked out on the use of this machine by trained personnel before operating equipment! Also, please communicate with other users when evaporation of a non-routine material is desired as its presence in the system may interfere with the devices of others!

3.1 Starting up from STANDBY mode

1. Before starting, make sure that the mechanical and diffusion pumps have been working at least for 1 hour.

2. Write down legibly your name, the date, and what material you are evaporating in the log book.

3. The machine settings should follow the table below:

Mode	STBY
Bell Jar	Firmly down
Mechanical Pump	ON
Diffusion Pump	ON
Ion Gauge	OFF
Degassing	OFF
Foreline Pressure	Less than 100 mTorr
Rough Line Pressure	Less than 500 mTorr
Cooling Water	Running

   If any item is out of the above specifications call the key operator.

4. Add liquid nitrogen to the cold trap (large funnel at rear of machine). After a few minutes, add more. Continue until you see liquid emerge from the overflow hose at the rear left of the machine. Wait about 30 min.

5. Switch the single lever knob to VENT.

6. Open the nitrogen vent line valve slightly and hold it open until the chamber is completely vented. (If the valve is simply opened all the way, the high pressure of the line can cause unwanted disturbance inside the vacuum chamber.)

7. Turn off the nitrogen vent line.

8. Lift bell jar carefully. If you want to keep the bell jar open for a while, put the single lever knob to STBY.

   - NOTE: For lower ultimate pressure, minimize exposure to humid atmospheric air. Also, when placing samples and boats in position use gloves!

9. Load samples, masks, and material in positions 2 and 3. When material is loaded but bell jar is not going to be closed immediately, put a micro-glass over the boats for protecting the material.

10. If using the thickness monitor, remove the glass plate from under the monitor.

11. Ensure that all areas around the sample are covered with glass plates to prevent material from being deposited on the bell jar.

12. Inspect bell jar gasket and sealing surface for foreign particles.
13. Lower bell jar carefully. Make sure of the contact between the gasket of the bell jar and evaporator.
14. Switch knob to ROUGH.
    - If you hear noisy mechanical pumping sound more than 10 sec, adjust bell jar position in order to seal the leaking.
    - The Foreline pressure will start to rise as indicated by the Foreline thermocouple guage.
    - CAUTION: Do not allow the Foreline pressure to rise above 100 mTorr. If for some reason a longer roughing time is required, rotate control arm to STBY until the diffusion pump foreline pressure recovers, then go back to the ROUGH position to complete the roughing cycle.
15. Pump until 50-100 mTorr. (Don't leave in this position too long. If roughing line does not fall into this range within 15 min, put system into STBY mode and call key operator.)
16. Add liquid nitrogen if needed.
17. Switch knob to HI-VAC (high vacuum).
18. Turn on filament on high vacuum ionization gauge when pressure falls down (1 E-4 range).
19. Evaporation can commence once ~1 micron is reached.

3.2 Evaporation

1. When using thickness monitor, ensure that the proper density and impedance are set.
2. Make sure the shutter is in the closed position.
3. Plug the current cord into the hole corresponding to the boat number desired for evaporation.
4. Turn on the evaporation power supply.
5. Slowly increase the voltage until a rate appears on the thickness monitor.
6. When the desired evaporation rate is achieved, reset the thickness monitor and open the shutter.
7. When desired thickness is achieved (or material runs out), close the shutter, stop the thickness monitor, and reduce the voltage slowly.
8. Turn off power supply and unplug current cord. If material from another boat is to be evaporated, repeat the relevant steps above.
9. Turn off ionization guage filament current.
10. Put knob to STBY and leave it there for some minutes in order to allow the system to cool down.
    - While waiting, write the thickness indicated by the thickness monitor after entry in the log book.

11. Put knob to VENT. Turn on nitrogen vent line and wait for complete vent. Turn off nitrogen vent line.
12. Lift bell jar carefully.
13. Remove sample and boats. If you used the thickness monitor, replace glass sheet under it.

3.3 Shutdown

1. Lower down bell jar carefully.
2. Rotate lever to ROUGH.
3. When roughing line pressure reaches 100 mTorr, switch to STBY mode. Wait a few sec, when the foreline valve light turns on (click sound), your job is done.

DOCUMENT SOURCES:

Oregon State University Electrical and Computer Engineering Department

OSU ECE Materials and Device Group Training Documentation

Contributing Authors: Jeff Bender, John Ebner, Hyungmo Yoo, Tagore Kollipara and Leon Ungier

Documentation Owner: Professor John F. Wager